# PERFORMANCE EVALUATION OF EVACUATED TUBE SOLAR COLLECTOR USING WATER-BASED TITANIUM OXIDE ($TiO_2$) NANOFLUID

**M. Mahendran[1], Lee. G.C[1], K.V Sharma[1], and A. Shahrani [1]**

[1]Faculty of Mechanical Engineering
Universiti Malaysia Pahang, 26600 Pekan, Pahang, Malaysia
Email: mahen_mu@yahoo.com

## ABSTRACT

Experiments are undertaken to determine the efficiency of evacuated tube solar collector using water-based Titanium Oxide ($TiO_2$) nanofluid at Pekan campus (3˚32' N, 103˚25' E) Faculty of Mechanical Engineering, University Malaysia Pahang for conversion of solar thermal energy. Malaysia lies in the equatorial zone with an average daily solar insolation of more than 900 W/m² and can reach a maximum of 1200 W/m² for most of the year. Traditionally, water is pumped through the collector at an optimum flow rate, for extraction of solar thermal energy. If the outlet temperature of water is high, further circulation of water through the collector is useless. This is due to low thermal conductivity of water of 0.6 W/m.K compared to metals which is many orders higher. Hence, it is necessary to reduce the surface temperature either by pumping water at higher flow rate or by enhancing the fluid properties by dispersing with nanoparticles. Pumping water at higher flow rates is not advantageous as the overall efficiency of the system is lowered. Liquids in which nanosize particles of metal or their oxides are dispersed in a base liquid such as water are known as 'Nanofluid'. It results in higher values of thermal conductivity compared to the base liquid. The thermal conductivity increases with concentration and temperature of the nanofluid. The increase in thermal conductivity with temperature is advantageous for applications in collectors, as the solar insolation varies throughout the day, with a minimum in the morning reaching a maximum at 2.00p.m and reducing thereafter. The efficiency of the collector estimated using $TiO_2$ nanofluid of 0.3% concentration is about 0.73, compared to water which is about 0.58. The efficiency is enhanced by 16.7% maximum with 30-50nm size $TiO_2$ nanoparticles dispersed in water, compared to the system working with water. The flow rate is fixed at 2.7 litres per minute for both liquids.

***Keywords:*** Solar Energy, Nanofluid, Evacuated Tube Solar Collector

## INTRODUCTION

The solar radiation intensity in Malaysia varies due to high humidity and unpredictable weather, especially during the period of monsoon. It was observed by (Othman et al., 1993) that the instantaneous solar radiation intensity or insolation can reach as high as 1400 W/m² in Malaysia. Many parts of Malaysia have a short duration of sunshine hours. Hence, an efficient solar collector system for Malaysian conditions should be designed to absorb maximum heat with minimum convective loss.

Many researchers have concluded that systems employing Evacuated Tube Solar Collector (ETSC) have higher efficiencies compared to a conventional Flat Plate Collector (FPC) (Gordon and Society, 2001; Morrison et al., 2005; Badar et al., 2011).

The features of ETSC are rows of concentric glass tube assembly, placed parallel to each other, with vacuum between the tubes. The tubes are transparent to solar radiation for a wide range of wavelengths. The outer surface of the inner tube is coated with a selective material, to absorb maximum solar radiation. The fluid flows in the inner tube absorbing the thermal energy. The method of energy transfer can be direct or indirect depending on the design. In the indirect method, a secondary fluid transfers the heat to the working fluid with the aid of a heat exchanger. The secondary fluid can be water, liquid refrigerant or a nanofluid (Gordon and Society, 2001).

The nanofluids are engineered preparation of fluids by dispersing nanosize metal or metal oxide particles dispersed in a base liquid such as water. The nanofluids are observed (Choi and Eastman, 2001) to possess higher thermal conductivity. Hence higher heat transfer coefficients are obtained due to enhanced thermal properties compared to base liquid.

(Lee et al., 1999) found that the enhancement of thermal conductivity in a range of 7-30% when Aluminium Oxide ($Al_2O_3$) and Copper Oxide (CuO) nanoparticles were suspended with water and ethylene glycol in 1-5% particle volume fraction. Experiments are undertaken by (Pak et al., 1998) for the determination of forced convection heat transfer coefficients with 13nm $Al_2O_3$ and 27nm $TiO_2$ submicron particles dispersed in water. They observed heat transfer coefficients to increase with concentration.

In recent studies, the thermal conductivity enhancement of base liquids using carbon nanotubes (CNT) nanofluids were tested in solar collectors by (Natarajan et al., 2009). Hence, reported the efficiency of the conventional solar water increases if these fluids are used as a heat transport medium. The effect of nanofluids on the micro solar thermal collector was studied by (Otanicar et al., 2010). The solar thermal collectors have improved up to 5% efficiency by using nanofluids as the working fluid. (Yousefi et al., 2012) compared the efficiency of a FPC using water-based alumina nanofluids with and without Triton X-100 as surfactant. The results show that alumina nanofluids using the surfactant have improved the heat transfer of the system and enhanced efficiency up to 15.63%.

The present paper objective is to study the efficiency of ETSC using water-based TiO2 nanofluid as the working fluid compared to base fluid. Hence, predict the efficiency of ETSC using water-based $Al_2O_3$ with the experimental data.

## EXPERIMENTAL SETUP

The schematic diagram of the experimental system is shown in figure 1, and the actual photograph of the experimental system is shown in figure 2. The experimental apparatus of the solar system mainly consisted with a 16-tubes ETSC module, a digital flow rate meter, a thermocouple monitor, an air-cooled heat exchanger, an electrical water pump, a solar meter and a power supply.

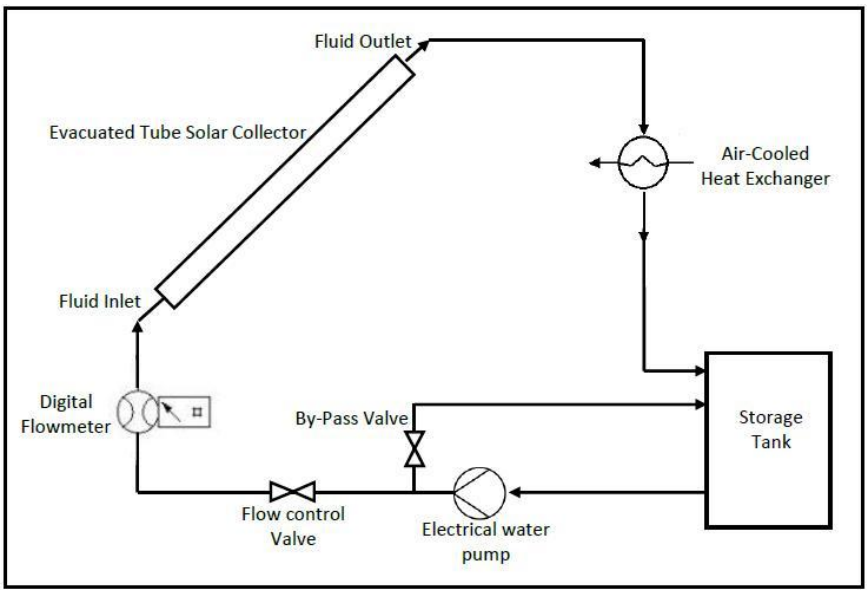


Figure 1. The schematic diagram of the experimental system

The specifications of ETSC that used in this experiment are given in Table 1. The digital flowmeter with two decimal reading values ranged from 1.00 to 10.00 litre per minute (LPM). The solar collector was tilted with an optimum angle of 8.2˚ facing due south based on the calculation method suggested by (Nayak, 2008). Global solar radiation was measured with portable solar meter which is ranged from 0 to 1200 W/m². The inlet and outlet temperatures of fluid that enters and leaves the solar collector and surrounding ambient temperature are monitored at 3 channels with thermocouple monitor. An air-cooled heat exchanger used to dissipate heat from the hot fluids that leave the collector. The electrical water pump with 0.5Hp has maximum flowrate about 14.0 LPM in shown Figure 1. The storage tank has a capacity of 8.0 litres and is connected to an electrical pump. The fluid pumped to the system at an optimum flowrate 2.5 LPM for distilled water remained constant throughout the experiment. Experiments are undertaken at flow rates of 2.0, 2.7, 3.0 and 3.5 LPM. From the graph drawn between temperature differences versus insolation for various flow rates, it is observed that a flow rate of 2.5 LPM has given maximum temperature difference. The cooled return fluid from the solar collector and bypass valve are connected to the storage tank. The system is a closed loop as shown in Figure 1. The fluid mass flowrate was controlled using the flow-control valve where the bypass valve was kept open normally.

Table 1. The specification of Evacuated tube Solar Collector

| **Specification** | **Dimension / Material** | **Unit** |
|---|---|---|
| Length x Width x Height | 2126 x 1920 x 150 | mm |
| Absorber Area | 2.77 | m² |
| Gross Area | 4.08 | m² |
| Weight | 100 | kg |
| Glass Material | Borosilicate Glass | - |
| Glass tube diameter | 100 | mm |

| | | |
|---|---|---|
| Wall thickness | 2.5 | mm |
| Transmittance | > 0.90 | - |
| Absorptance | > 0.92 | - |
| Emittance | < 0.08 | - |
| Absorber Material | Aluminium | - |
| Selective Coating | Aluminium Nitride | - |
| Header box Material | Aluminium | - |
| Header box Size | 1918 x 108 x 126 | mm |
| Pressure Drop per module | <20 | mbar |

All the measuring instruments were calibrated before the conduct of the experiment. The digital flow rate was calibrated with the aid of a measuring jar. The test was repeated several times to ensure that the readings are within the acceptable range of less than 1% variation. The thermocouple monitor temperatures reading are checked and compared with portable thermocouple device which has valid calibrated certificate to verify the readings are the equivalent.

Figure 2. The actual photograph of the experimental system

***Material***

The commercial $TiO_2$ nanopowder dispersion with 40 weight percent was used in this experiment. It has 99.5% of purity and average particle size 30-50nm. Nanoparticle dispersions are suspensions of nanoparticles in water. The $TiO_2$ nanopowder dispersion diluted with distilled water were used during the study as a base fluid. The physical properties of nanoparticles that used in the present experiment and analysis are given in Table 2.

Table 2. Physical properties of nano materials

| Nanoparticle | Thermal Conductivity, W/m.K | Density, kg/m$^3$ | Specific heat, J/ kg.K | References |
|---|---|---|---|---|
| $TiO_2$ | 8.4 | 4175 | 692 | (Pak and Cho, 1998) |
| $Al_2O_3$ | 36 | 3880 | 773 | (Pak and Cho, 1998) |

***Preparation of nanofluid***

The two-step method used to disperse $TiO_2$ nanopowder into the distilled water. The two-step method is a better method for preparation of metal or metal oxide nanofluids. It has an advantage of reduced agglomeration (Zhu et al., 2004; Hwang et al., 2006; Das, 2007). A measured quantity of $TiO_2$ nanopowder, is dispersed in distilled water, to obtain 0.3% volume percent, $\varphi$ nanofluid. The nanofluids are dispersed with the aid of a mechanical stirrer shown in Figure 3 for about 2 hours to achieve a homogenously dispersed solution.

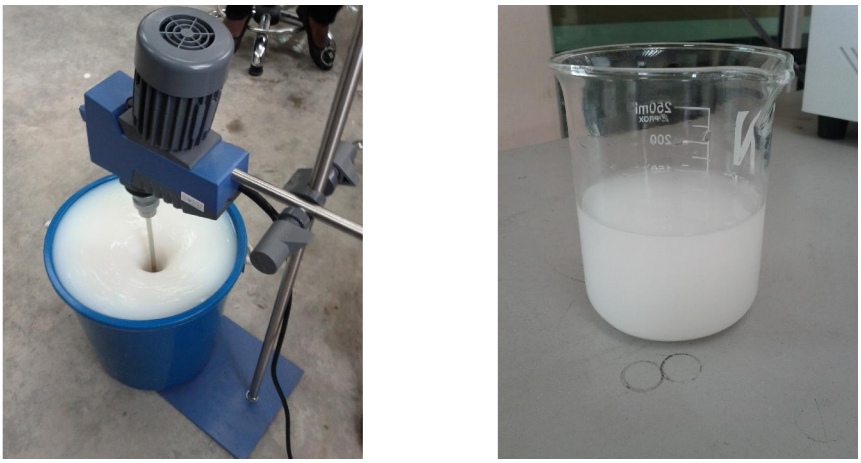

(a) Stirred $TiO_2$ nanofluid (b) Prepared $TiO_2$ nanofluid

Figure 3. Titanium Oxide nanofluid preparation

The concentration in weight percentage, $\omega$ is converted into volume percentage, $\varphi$ with Equation (1) using the nanoparticle density listed in Table 2. The volume of distilled water to be added $\Delta V$ for attaining a desired concentration $\varphi_2$ can be estimated with Equation (2) with the initial conditions of $V_1$ and $\varphi_1$.

$$\varphi = \frac{\omega \rho_w}{\left(1 - \frac{\omega}{100}\right)\rho_p + \frac{\omega}{100}\rho_w} \quad \text{where } \omega = \left[m_p / \left(m_p + m_w\right)\right] \times 100 \tag{1}$$

$$\Delta V = \left(V_2 - V_1\right) = V_1\left(\frac{\varphi_1}{\varphi_2} - 1\right) \tag{2}$$

***Determination of Specific Heat Capacity of Nanofluid***

(Zhou et al., 2010) compared the specific heat capacity of CuO or Ethylene Glycol (EG) nanofluid at different volume concentrations obtained through experiments with Equation (3). The experimental values decreased from 2550 to 2450 J/kg.K with an increase in volume concentration from 0.1 to 0.6%. The experimental values are higher than the values calculated with Equation (3) developed on the law of mixtures.

$$C_{nf} = \frac{(1-\phi)(\rho\, C)_w + \phi\,(\rho C)_p}{(1-\phi)\rho_w + \phi\rho_p} \tag{3}$$

***Collector Thermal Performance Testing Method***

The thermal performance for ETSC was tested under ASHRAE / ASNI Standard 93-2003. This standard also can be used to determined thermal performance of FPC and Concentrating Solar Collector (CSC). The instantaneous efficiency at different combinations of solar insolation, ambient temperature, and fluid inlet temperature are obtained to determine the thermal performance of the collector.

The test data were measured when the system maintains for a period of 15 minutes at steady-state or quasi-steady state condition as permitted deviation of measured parameters during a period as listed in Table 3. After a steady-state or quasi-steady state condition was maintained, the data were measured at an interval of 15 minutes from 9.00a.m until 6.00p.m. The invalid data which is not at steady-state or quasi-steady state condition were ignored.

Table 3. Permitted deviation of measured parameters during a period

| **Parameter** | **Deviation from the mean** | **Unit** |
|---|---|---|
| Total Solar Insolation, $G_T$ | ± 50 | W/m² |
| Ambient temperature, $T_a$ | ± 1 | K |
| Wind speed, $V_w$ | 2 – 4 | m/s |
| Fluid mass flowrate, $\dot{m}$ | ± 1 | % |
| Collector fluid inlet temperature, $T_i$ | ± 0.1 | K |

***Efficiency of ETSC***

The useful energy was determined using Equation (4), with measured value of inlet and outlet fluid temperatures and fluid mass flowrate. The specific heat capacity was determined using Equation (3). The useful energy can also be expressed in terms of

the energy absorbed by the collector and the energy lost to the surrounding as given by Equation (5) (Duffie and Beckman, 2006).

$$Q_u = \dot{m} C_p (T_o - T_i) \tag{4}$$

and

$$Q_u = \dot{m} \frac{C_p (T_o - T_i)}{A \cdot G_T} \tag{5}$$

## RESULTS AND DISCUSSION

The solar insolation, $G_T$ is an important parameter to evaluate the efficiency of the collector. It is dependent to the geographic location, weather and climate. In the present experiment, weather conditions such as passing cloud, cloudy sky, rain and etc influence solar insolation values. Figure 4 and Figure 5 show the typical solar insolation against time on a clear sky and cloudy day respectively.

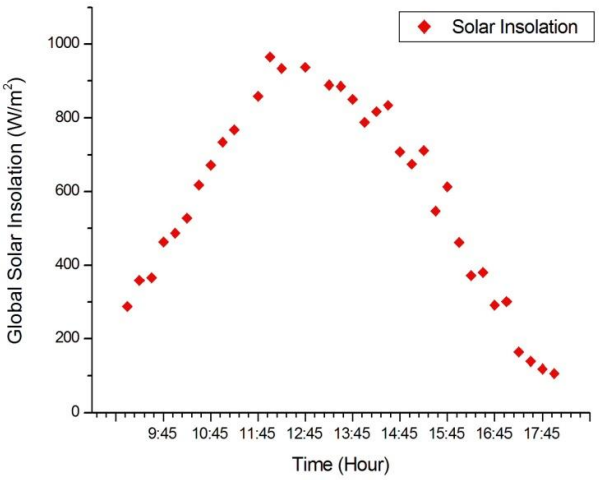


Figure 4. Solar Insolation against time on a clear sky day

It was observed for a clear sky day the variation of solar insolation to be parabolic with the maximum reaching at about 2.00p.m. The maximum insolation on the tilted surface of ETSC was about 958 W/m² on that particular day. Nevertheless, on a cloudy day, the solar insolation as irregular pattern, the solar insolation rise and drop along the day according to the clouds. The maximum recorded insolation was 630 W/m². Therefore, the steady or quasi steady state condition was difficult to achieve on such worst weather conditions and the testing was only conducted on the clear sky day.

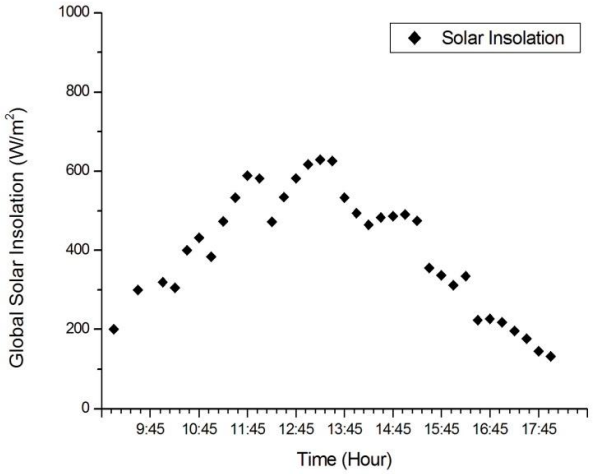


Figure 5. Solar Insolation against time on a cloudy day

Experimental data on the clear sky day were tabulated according to solar insolation incident at the site. The temperatures at the inlet and outlet of the setup are recorded for water and nanofluid. The temperature difference between the inlet and outlet is then estimated. An average value for an insolation is considered in the analysis after a repeated number of tests. The data for water and nanofluid are shown plotted in figure 6.

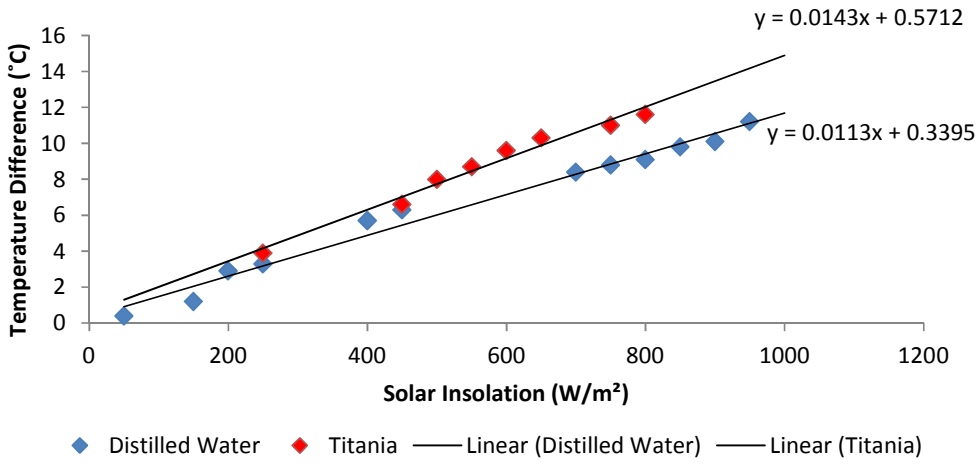


Figure 6. Average Temperature difference of water and 0.3% Titanium Oxide ($Ti0_2$) against solar insolation ($W/m^2$)

Based on the figure 6, nanofluid and water temperature difference are directly proportional to the solar insolation. $TiO_2$ nanofluid has a higher temperature difference than water. The presence of $TiO_2$ nanoparticles enhances the thermal properties compared to water. These enhancements increase the capability to transfer heat from the absorber plate to the working fluid. The heat transfer capability of nanofluid increases with solar insolation availability. It means the nanofluids have the ability to absorb heat at higher solar insolation levels and perform better at higher temperatures compared to water. From the Figure 6, statistical analysis is performed water and nanofluid. The equations from the statistical analysis are used estimated the temperature difference for other range of solar insolation. The temperature difference of nanofluid increased by 19.0% maximum compared to water.

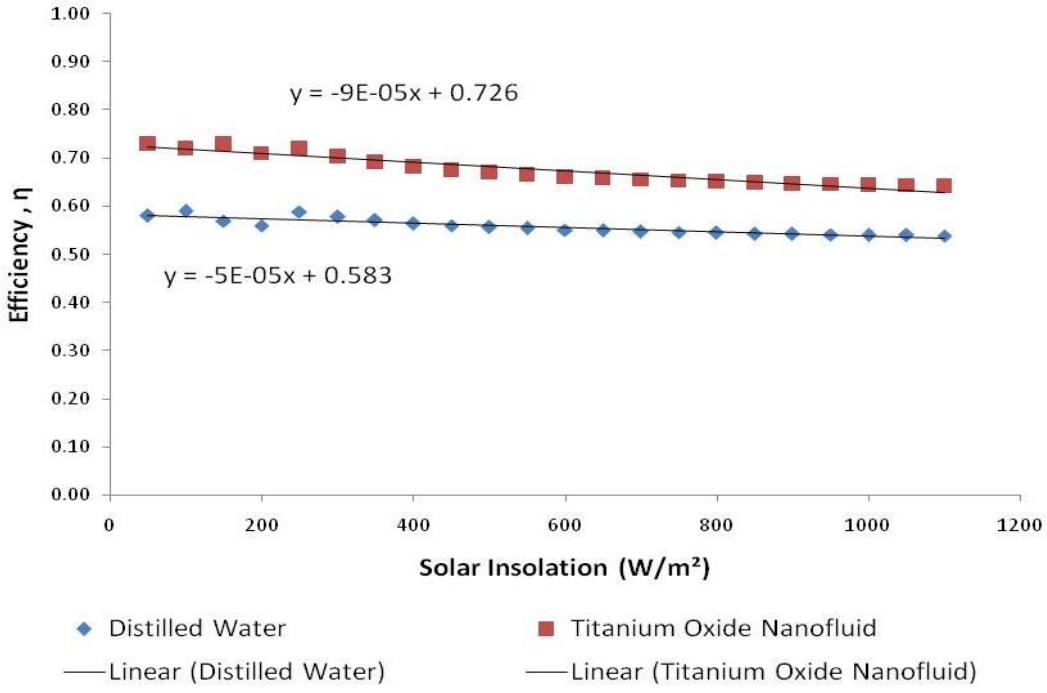


Figure 7. Efficiency of water and 0.3% Titanium Oxide ($TiO_2$) against solar insolation ($W/m^2$)

The instantaneous efficiency was determined using the Equation (5) for the experimental data and shown as Figure 7. The mass flowrate of the system was kept constant throughout the experiment for water and $TiO_2$ nanofluid. The specific heat capacity of $TiO_2$ nanofluid was determined using the Equation (3). The aperture area of collector was the absorber area for solar energy. From figure 7, the efficiency of $TiO_2$ nanofluid is higher than water, where the maximum efficiency is 0.73 and 0.58 respectively. The efficiency of the system using 0.3% $TiO_2$ nanofluid has increased by 16.67% compared to water. the system using water-based $Al_2O_3$ nanofluid is predicted to have 8% higher efficiency compared to water-based $TiO_2$ nanofluid because of its higher thermal conductivity.

## CONCLUSION

The temperature rise of nanofluid is 19.0% higher than water at the exit of the collector. The maximum efficiency of the system using 0.3% $TiO_2$ nanofluid is 0.73, and distilled water is 0.53. The efficiency of the system has increased by 16.67% compared to its based liquid. The greater the solar insolation, the higher the temperature difference achieved, for $TiO_2$ nanofluid. The ETSC system using water-based $Al_2O_3$ nanofluid is predicted to have 8% higher efficiency compared to water-based $TiO_2$ nanofluid.

## REFERENCES


Badar, A. W., Buchholz, R. and Ziegler, F. 2011. Experimental and theoretical evaluation of the overall heat loss coefficient of vacuum tubes of a solar collector. Solar Energy, 85(7): 1447-1456.

Choi, S. U. S. and Eastman, J. A. 2001. Enhancing thermal conductivity of fluids with nanoparticles.

Das, S. K. 2007. Nanofluids: Science and Technology: Wiley-Interscience Publication.

Duffie, J. A. and Beckman, W. A. 2006. Solar Engineering of Thermal Processes: Wiley-Interscience Publication.

Gordon, J. and Society, I. S. E. (2001). Solar Energy: The State of the Art: ISES Position Papers, James & James.

Hwang, Y. J., Ahn, Y. C., Shin, H. S., Lee, C. G., Kim, G. T., Park, H. S. and Lee, J. K. 2006. Investigation on characteristics of thermal conductivity enhancement of nanofluids. Current Applied Physics, 6(6): 1068-1071.

Lee, S., Choi, S. U. S., Li, S. and Eastman, J. A. 1999. Measuring thermal conductivity of fluids containing oxide nanoparticles. Journal of Heat Transfer, 121(2): 280-289.

Morrison, G. L., Budihardjo, I. and Behnia, M. 2005. Measurement and simulation of flow rate in a water-in-glass evacuated tube solar water heater. Solar Energy, 78(2): 257-267.

Natarajan, E. and Sathish R. 2009. Role of nanofluids in solar water heater. The International Journal of Advanced Manufacturing Technology: 1-5.

Nayak, S. P. S. J. K. 2008. Solar Energy: Principles of Thermal Collection and Storage. Tata McGraw-Hill Publishing Co.

Otanicar, T. P., Phelan, P. E., Prasher, R. S., Rosengarten, G. and Taylor, R. A. 2010. Nanofluid-based direct absorption solar collector. Journal of Renewable and Sustainable Energy, 2(3): 033102-033113.

Othman, M. Y. H., Sopian, K., Yatim, B. and Dalimin, M. N. 1993. Diurnal pattern of global solar radiation in the tropics: A case study in Malaysia. Renewable Energy, 3(6–7): 741-745.

Pak, B. C. and Cho, Y. I. 1998. Hydrodynamic and heat transfer study of dispersed fluids with submicron metallic oxide particles. Experimental Heat Transfer, 11(2): 151-170.

Yousefi, T., Veysi, F., Shojaeizadeh, E. And Zinadini, S. 2012. An experimental investigation on the effect of $Al_2O_3$–$H_2O$ nanofluid on the efficiency of flat-plate solar collectors. Renewable Energy, 39(1): 293-298.

Zhou, L.P., Wang, B.X., Peng, X.F., Du, X.Z. and Yang, Y.P. 2010. On the specific heat capacity of CuO nanofluid. Advances in Mechanical Engineering.

Zhu, H.T., Lin, Y.S. and Yin, Y.s. 2004. A novel one-step chemical method for preparation of copper nanofluids. Journal of Colloid and Interface Science, 277(1): 100-103.